Current Biology, Vol. 12, 876–884, June 4, 2002, ©2002 Elsevier Science Ltd. All rights reserved. PII S0960-9822(02)00864-3

Zebrafish Rho Kinase 2 Acts Downstream of Wnt11 to Mediate Cell Polarity and Effective Convergence and Extension Movements

Florence Marlow, Jacek Topczewski, Diane Sepich, and Lilianna Solnica-Krezel[1]
Department of Biological Sciences
Vanderbilt University
VU Station B 351634
Nashville, Tennessee 37235-1634

Summary

Background: During vertebrate gastrulation convergence and extension (CE), movements narrow and lengthen embryonic tissues. In *Xenopus* and zebrafish, a noncanonical Wnt signaling pathway constitutes the vertebrate counterpart to the *Drosophila* planar cell polarity pathway and regulates mediolateral cell polarization underlying CE. Despite the identification of several signaling molecules required for normal CE, the downstream transducers regulating individual cell behaviors driving CE are only beginning to be elucidated. Moreover, how defective mediolateral cell polarity impacts CE is not understood.

Results: Here, we show that overexpression of zebrafish dominant-negative Rho kinase 2 (dnRok2) disrupts CE without altering cell fates, phenocopying noncanonical Wnt signaling mutants. Moreover, Rho kinase 2 (Rok2) overexpression partially suppresses the *slb/wnt11* gastrulation phenotype, and ectopic expression of noncanonical Wnts modulates Rok2 intracellular distribution. In addition, time-lapse analyses associate defective dorsal convergence movements with impaired cell elongation, mediolateral orientation, and consequently failure to migrate along straight paths. Transplantation experiments reveal that dnRok2 cells in wild-type hosts neither elongate nor orient their axes. In contrast, wild-type cells are able to elongate their cell bodies in dnRok2 hosts, even though they fail to orient their axes.

Conclusions: During zebrafish gastrulation, Rok2 acts downstream of noncanonical Wnt11 signaling to mediate mediolateral cell elongation required for dorsal cell movement along straight paths. Furthermore, elongation and orientation of the cell body are independent properties that require both cell-autonomous and nonautonomous Rok2 function.

Introduction

During vertebrate gastrulation, massive cell rearrangements generate the three germ layers and shape the embryonic body [1]. In the dorsal-lateral regions of the frog and in dorsal regions of zebrafish, gastrula cells intercalate among mediolateral (ML) neighbors to drive the narrowing in dorsoventral (convergence) and simultaneous anteroposterior lengthening (extension) of embryonic tissues [1, 2]. Convergent extension movements driven by intercalation involve and are dependent on ML cell elongation [3], such polarization likely requires reorganization of the cytoskeleton and modulation of cell adhesion.

Recent investigations in the frog and analysis of zebrafish gastrulation mutants implicate a noncanonical Wnt signaling pathway similar to the *Drosophila* planar cell polarity (PCP) pathway in regulating polarized cell behaviors required for CE [4–6]. As in *Drosophila*, Frizzled Wnt receptors (Fz) and Dishevelled (Dsh) mediate intracellular transduction of tissue polarity signaling [6–8]. In vertebrate gastrulae, Wnt11/Slb glycoprotein ligand and membrane associated Glypican (Knypek) act as components of this pathway [4, 5, 9]. Mutations in zebrafish *silberblick/wnt11* (*slb*) and *knypek* (*kny*) genes impair convergence and extension without altering cell fates [4, 5]. Similar impairment of CE is observed in *Xenopus* and zebrafish when other noncanonical Wnts (Wnt5 or Wnt4), dominant-negative Frizzled receptors, or a truncated Dishevelled that specifically blocks noncanonical signaling are overexpressed [4, 9–13]. A novel formin homology protein, Daam1, in vertebrates and small GTPases, including Cdc42 and RhoA, have been identified as transducers of tissue polarity signals that act downstream of Dsh in *Drosophila* and during vertebrate gastrulation [14–16].

Recently, *Drosophila* Rho-associated kinase (Drok), a serine threonine kinase RhoA effector, was shown to regulate some aspects of planar polarity in eye and wing disc cells downstream of Fz and Dsh [17]. Binding to activated GTP-RhoA results in activation of cytosolic Rok2, which becomes membrane associated and phosphorylates target proteins [18]. Drok phosphorylation and activation of nonmuscle myosin II regulatory light chain (MRLC) restricts actin bundle formation in the wing [17]. During nematode embryonic body elongation, Rok2 homolog (Let 502) regulates hypodermal cell shape changes by inhibiting smooth muscle myosin phosphatase activity and increasing MRLC activation [19]. In vertebrates, Rok2 function has recently been implicated in organ morphogenesis; inhibition of Rok function in neurulating chick and murine embryos results in cardiabifida, a defect associated with impaired migration and failure of cardiac progenitor cell fields to fuse [20]. Moreover, dominant-negative Rok2 disrupts the actin cytoskeleton and inhibits carcinoma cell migration in culture [18, 21], implicating Rok in cell movement.

Despite the connection between Rok2 and cell motility, whether it regulates cell behaviors underlying vertebrate gastrulation remains unexplored. Here we show that Rok2 function is required for normal convergence and extension movements in the zebrafish gastrula. Overexpression of dominant-negative Rok2 (dnRok2) impairs convergence movements by disrupting cells' elongation and orientation along ML embryonic axis and, consequently, their ability to move dorsally along straight paths. In vivo mosaic analyses reveal that Rok2 has cell-autonomous and nonautonomous roles in cell polarization and that elongation of the cell body is inde-

[1]Correspondence: lilianna.solnica-krezel@vanderbilt.edu

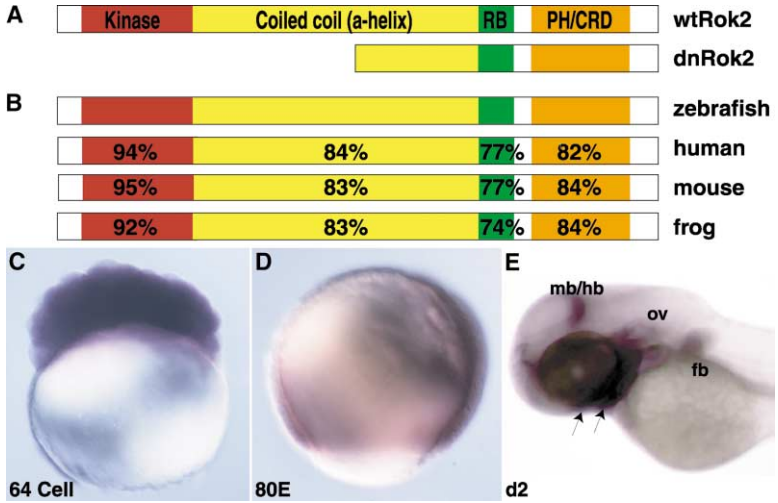

Figure 1. Zebrafish *rok2* Is Maternally and Zygotically Expressed

(A) Predicted protein domains and a truncated construct encoding a putative dominant-negative Rok2 designed based on (B) the similarity between Rok2 sequences from other vertebrates. Rok2 is uniformly expressed at (C) 64 cell. (D) At 80%, epiboly transcripts are ubiquitous. (E) At 2 days, *rok2* is localized to the midbrain-hindbrain boundary (mb/hb) in the brain, the otic vesicles (ov), arches that will contribute to the jaw (arrows), and the fin buds (fb). (C–E), lateral views. hp, head process; tb, tailbud.

pendent from its ML orientation. Finally, we show that Rok2 overexpression can suppress the *slb* mutant gastrulation phenotype, and noncanonical Wnts modulate Rok2 intracellular distribution. We propose that Rok2 acts downstream of Slb/Wnt11 in mediating ML cell elongation and orientation required for effective convergence and extension movements.

Results and Discussion

Rok2 Is Ubiquitously Expressed during Early Zebrafish Embryogenesis

To examine Rok2 function during vertebrate gastrulation, we cloned the zebrafish *rok2* gene. The predicted protein encoded by the full-length zebrafish gene is highly similar to Rok2 from other vertebrates and includes all the formerly characterized functional domains (Figure 1B).

Examination of *rok2* expression reveals maternal transcripts in all cells at early cleavage stages (Figure 1C and data not shown). Expression persists in all cells during blastula stages and during gastrulation (Figure 1D and data not shown). By 2 days postfertilization, expression becomes highly restricted to the midbrain/hindbrain boundary, the branchial arches, the otic vesicles, and fin buds (Figure 1E).

Interference with Rok2 Function Disrupts CE without Altering Cell Fates

Previous studies demonstrated that the carboxy-terminal region of mammalian Rok negatively regulates kinase activity residing in the amino terminus [18, 22]. Evidence for this model of regulation is based on observations from cell culture studies where carboxy-terminal portions of Rok2 bind and inactivate the kinase domain in a dominant-negative fashion dependent on the pleckstrin homology (PH) and Rho binding domains (RB) [23]. Hence, we addressed the role of Rok2 during gastrulation by deleting the amino terminus including the kinase domain to generate a putative dominant-negative zebrafish protein.

At the end of gastrulation, wild-type (WT) embryos have elongated AP and narrow ML axes (Figures 2A and 2B). Additional axis elongation is observed during sementation stages (Figures 2C and 2D) [24, 25]. In contrast, embryos expressing synthetic RNA encoding zebrafish dnRok2 exhibited shortened AP axes and broader notochords and somites than control siblings, suggesting impaired CE movements (Figures 2E–2G). Similar gastrulation defects were observed when a rat dominant-negative point mutant construct, RokK112A, which abolishes kinase activity and behaves as a dominant-negative in cell culture, was overexpressed (Figure 2H) [18]. At 3 days postfertilization, embryos injected with *dnrok2* RNA remained shorter than control siblings, and some exhibited synopthalmia or cyclopia (Figure 2I).

To identify tissues affected by interference with Rok2 function, we analyzed the expression of cell- and tissue-specific genes by whole mount in situ hybridization. Expression of *distal-less3* (*dlx3*), marking the neuroectoderm boundaries, and *no tail* (*ntl*), in the nascent notochord, revealed a ML broader neural plate and notochord in dnRok2 expressing embryos compared to control siblings during early segmentation (Figures 2J–2N). Notochord abnormalities, including bifurcation of the axial domain, were observed with low frequency (Figure 2N). In addition, prechordal plate, marked by *hatching gland 1* (*hgg1*) expression, is positioned more posteriorly with respect to the anterior edge of the neural plate in injected embryos and is frequently abnormally elongated (Figure 2N). The penetrance of these defects among the injected embryos increased in a dose-dependent manner (Figure 2O). Coinjection of RNA encoding full-length Rok2 with *dnrok2* RNA suppressed neural plate, notochord, and prechordal plate CE defects in a dose-dependent manner, indicating that they arose due to specific interference with Rok2 function (Figure 2O). In addition, the point mutant construct rat RokK112A produced the same CE phenotype as determined by in situ hybridization and morphological criteria, supporting the specificity of the defects to interference with Rok2 function (Figure 2) [18]. Attempts to interfere with Rok2 using morpholino oligonucleotides were not successful, possibly due to abundant maternally deposited protein (Experimental Procedures and data not shown). At the doses used for this study, dnRok2-expressing embryos

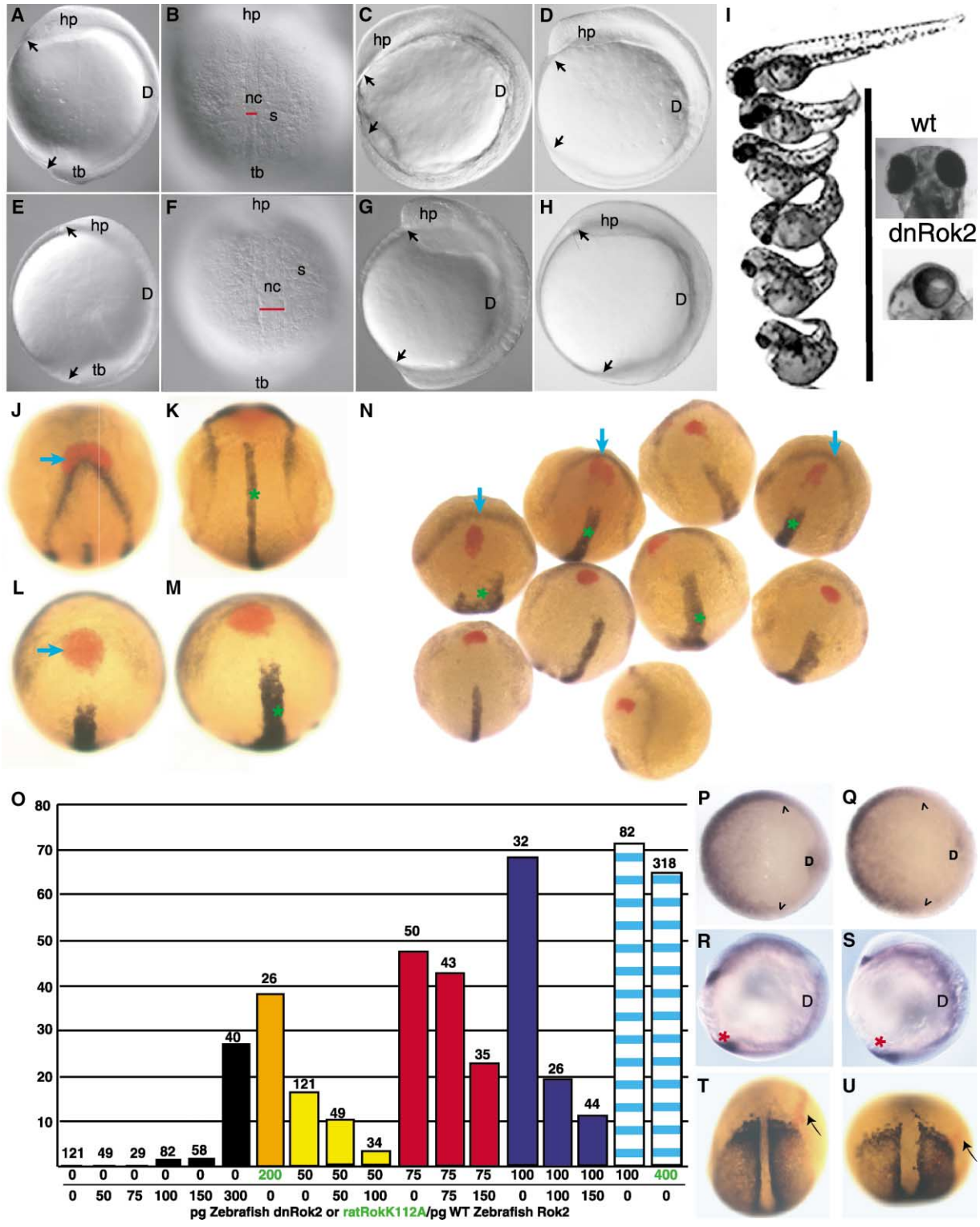

Figure 2. dnRok2 Disrupts Convergence Extension without Affecting Cell Fates

(A) The 2 somite stage WT embryo has an elongated anterior-posterior (AP) axis (arrows indicate the most anterior and posterior extent of the axis) and (B) exhibits a narrow and elongated notochord (nc). At 5 (D) and 8 somites (C), considerable extension of the AP axis is noted (arrows). In contrast, (E) embryos injected with zebrafish dnRok2 show shortened axis compared to WT and (F) have a shorter broader notochord (nc). (G) The shortening of the embryonic axis persists at the 8 somite stage. (H) This shortened phenotype is also observed when dominant-negative rat RokK112A is overexpressed. (I) At day 3, dnRok2-expressing embryos remain shorter and exhibit cyclopia (lower inset). (J) In WT, the anterior-most prechordal plate *hgg1* (red) is positioned rostral to *dlx3* expression in the periphery of the neural plate (arrows), and (K) *ntl* is expressed in the ML narrowed notochord (*). (L) In embryos expressing dnRok2, *hgg1* is caudal to a ML broader neural plate

complete epiboly comparable to WT, and mesoderm is properly formed. Doses of zebrafish dnRok2 above 300 pg/embryo resulted in abnormal cell divisions and arrested development prior to completion of gastrulation; both the cell division defects and early lethality were suppressed in a dose-dependent manner by injecting full-length Rok2 (data not shown). Therefore the doses, which interfere with CE, likely represent partial loss of Rok2 function, and at higher doses dnRok2 may affect additional proteins. Similarly, interference with cytokinsesis has been reported for both *Xenopus* and mammalian cells and for the Rok2-related yeast Orb2 protein [26, 27]. While overexpression of zebrafish Rok2 in WT embryos had no effect at low doses, high doses resulted in axial mesoderm and neural plate morphogenesis defects similar to those caused by dominant-negative dnRok2 overexpression at low penetrance. This indicates that CE is sensitive to both loss and gain of Rok2 function (Figure 2O). Therefore, we conclude that Rok2 function is required for normal CE.

Similar impairment of CE is associated with excessive BMP signaling or mutations in noncanonical Wnt signaling pathway components [4, 5, 28]. To test whether dorsoventral patterning is affected in dnRok2-expressing embryos, we analyzed the expression of *bmp4*, an indicator of ventral fate [29]. Expression of the *bmp4* gene was not significantly altered during early gastrulation ($n = 21$) or segmentation stages ($n = 68$) in dnRok2-expressing embryos compared to WT (Figures 2P–2S). Furthermore, lineage tracing experiments revealed that labeled lateral cells (positioned 90° from the dorsal embryonic shield) adopt similar fates in WT and dnRok2-expressing embryos (WT, $n = 2$ [25]; dnRok2, $n = 4$) (Figures 2T and 2U). Together, these results support the notion that altered cell fate does not account for the CE defect in dnRok2-expressing embryos.

Rok2 Is Required for Efficient Dorsal Convergence Movement

Previous studies of small cell populations have demonstrated that there are three domains of CE movements in zebrafish gastrulae as cells move from lateral to dorsal, with peak translocation occurring during mid to late gastrulation [28]. To explore the cellular motility defect underlying the dnRok2 CE phenotype, Nomarski time-lapse analysis was performed, and the migration speeds and paths of individual paraxial mesodermal cells were determined for WT ($n = 40$ cells from 2 embryos) and dnRok2-expressing embryos during the reported period of peak dorsal translocation ($n = 40$ cells from 2 embryos; Figures 3A and 3B) [28]. At this time, mesodermal cells move as individuals rather than as a sheet, so by monitoring the position of the notochord it is possible to determine the paths and speeds for individual cells within the tissue [2, 30, 31]. Analysis of total cell speeds (accounting for movement in all directions) revealed that the dnRok2 cells move slower than WT cells (69% of WT speed; $p < 2.8 \times 10^{-3}$) (Figure 3C). Notably, the net dorsal speed of dnRok2-expressing cells (accounting for dorsal movement) is particularly compromised, representing only 31% of the WT net dorsal speed (Figure 3C; $p < 4.6 \times 10^{-13}$). Paraxial cells in WT embryos move toward dorsal in a direct fashion with little change of direction, and their dorsal movement is biased toward the animal or vegetal pole, dependent on their position relative to the gastrula equator as observed for zebrafish ectodermal cells (Figure 3D) [30]. In contrast, although the net paths of dnRok2-expressing cells are dorsally directed, these cells frequently change direction and consequently migrate less effectively toward dorsal (Figure 3E). Moreover, while the net paths of individual WT cells are similarly oriented with respect to the notochord (Figure 3F), the net paths of dnRok2-expressing cells are oriented more randomly to one another and the notochord (Figure 3G). Cumulatively, these results indicate that impaired dorsalward movement along straight paths underlies the dnRok2 CE defect. Preliminary analysis with membrane-localized GFP indicates that Rok2 is required to limit protrusive activity; thus, abnormal protrusive activity may contribute to the dnRok2 CE defect (F.M., J.T., and L.S.-K., unpublished data).

Rok2 Is Required for Mediolateral Cell Elongation during CE

CE of tissues is correlated with and requires that cells elongate their bodies and orient them mediolaterally [1, 5, 6, 30]. Using in vivo confocal microscopy, we measured the elongation and orientation of labeled paraxial ectoderm and mesodermal cells in WT and dnRok2-expressing embryos (Figures 4A and 4B). In WT embryos, 70% of ectodermal cells and 72% of mesodermal cells oriented their long axes within a $\pm$ 20° arc perpendicular to the notochord and exhibited average length-to-width ratios (LWR) of 2.0 $\pm$ 0.3 ($n = 54$) and 1.9 $\pm$ 0.3 ($n = 43$), respectively, indicating that these cells are highly elongated and mediolaterally oriented (Figures 4A, 4G, and 4H) [5, 28]. In contrast, only 30% ($p < 0.001$; $n = 66$) of dnRok2-expressing ectodermal and 37% ($p < 0.001$; $n = 164$) of dnRok2 mesodermal cells were ML oriented, and these cells were significantly less elongated with average LWRs of 1.5 $\pm$ 0.3 ($p < 3.9 \times 10^{-14}$; $n = 66$) and 1.5 $\pm$ 0.3 ($p < 4.3 \times 10^{-10}$; $n = 164$), respectively (Figures 4B, 4G, and 4H). The failure of paraxial cells to elongate and orient mediolaterally might underlie

(arrows), and (M) *ntl* expression reveals a shorter broader notochord (*). (N) Range of phenotypes observed in embryos injected with 75 pg *dnrok2* mRNA and hybridized as in (J); arrows indicate posteriorly positioned prechordal plate relative to the neural plate; * marks the notochord. The penetrance of CE defects increases with the dose of dnRok2. (O) The dnRok2 CE phenotype, embryos in which the prechordal plate (*hgg1*) was posterior to *dlx3* (solid bars), was suppressed by increasing amounts of full-length Rok2 in a dose-dependant manner (doses in green text indicate overexpression of ratRokK112A; all others are overexpressing zebrafish dnRok). Striped bars indicate CE phenotypes scored by shortened AP axes in live embryos. Cell fates are not changed, as expression of the ventral marker *bmp4* is comparable between (P and Q) wild-type and (R and S) dnRok2-expressing embryos at shield (^ indicates dorsal extent of expression; animal view) and later at 8S stage (* marks bud expression; lateral view), respectively. Labeled lateral cells adopt similar fates in (T) WT and (U) dnRok2-expressing embryos as indicated by relative position with respect to *papc* expression (arrows). "D" denotes dorsal.

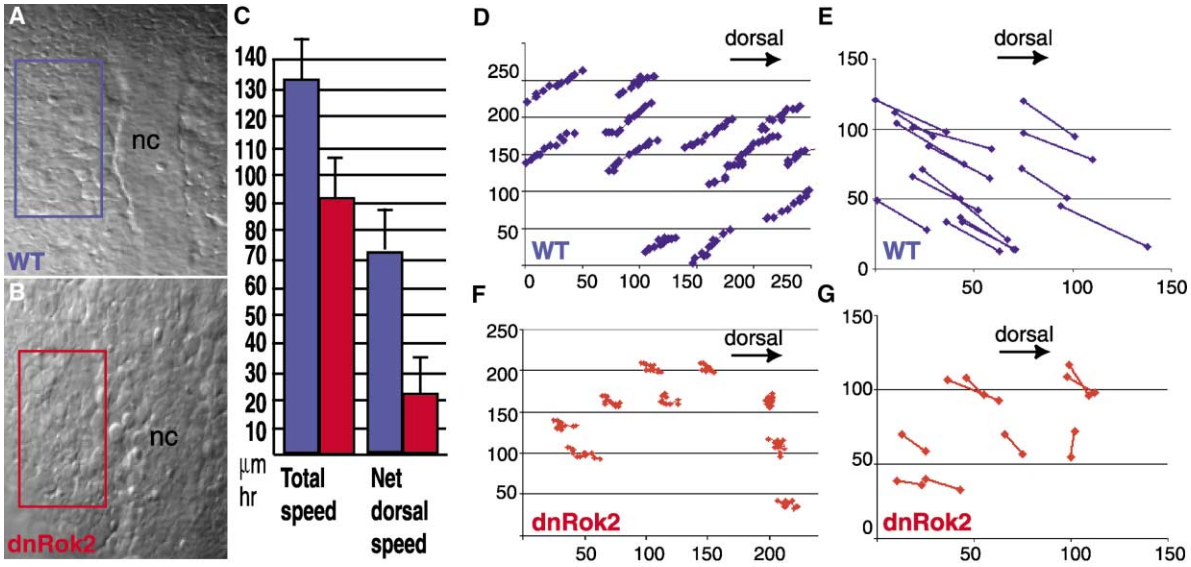

Figure 3. Rok2 Is Required for Migration along Straight Paths during CE

Dorsal views of (A) WT embryo and (B) dnRok2-expressing embryo at bud stage (boxes highlight the paraxial region, which was the focus of the cell orientation and migration analyses that follow). (C) WT cells (blue) migrate faster (μm/hr) than dnRok2-expressing cells (red) when total and net dorsal speeds are compared. Cell paths for (D) WT and (E) dnRok2-expressing paraxial cells extracted from Nomarski time-lapse images. Each point represents the center for the cell in pixels, where 50 pixels = 10.5 μm. (D) WT cells change direction less frequently than (E) dnRok2-expressing cells as they move dorsally (arrow). The net paths of individual cells are similarly oriented in (F) WT embryos and are less oriented in (G) dnRok2-expressing embryos (each graph shows representative data obtained from individual embryos).

the frequent direction changes observed during dorsal movement of these cells in dnRok2-expressing embryos. These observations help to understand how defective cell polarity impacts cell movement and CE in the context of whole embryos. Strikingly, the average elongation of dnRok2-expressing cells was similar whether or not cells were ML oriented (1.5 ± 0.31 among ML aligned cells, 1.5 ± 0.31 among nonaligned cells). Similarly, when the orientation of elongated cells (LWR ≥ 1.8) was measured, only 34% were found to exhibit ML-biased orientation, while 39% of cells with a LWR < 1.8 were ML oriented. This suggests that ML-biased orientation and cell elongation may arise independently.

Cell Orientation and Elongation Are Independent Properties Requiring Both Cell Autonomous and Nonautonomous Rok2 Functions

We used cell elongation and orientation as the basis for testing the cell autonomy of Rok2 function. Labeled cells were transplanted from donors injected with rhodamine-dextran lineage tracer alone or with *dnrok2* RNA to unlabeled WT or dnrok2-expressing hosts (Figure 4C) [5]. ML orientation and cell elongation were not significantly different between ectoderm and mesoderm for WT ($p > 0.18$ for LWR and $p > 0.2$ for ML alignment) or dnRok2-expressing embryos ($p > 0.99$ for LWR and $p > 0.5$ for ML alignment) at this stage of development; therefore, these cell populations were pooled for cell transplantation studies. Labeled WT cells transplanted to WT hosts were elongated (LWR = 1.9) and exhibited ML-biased orientation (74%) comparable to those observed for DiI-labeled cells, indicating that the transplantation procedure does not impair cell elongation or orientation ($p > 0.74$ for LWR and $p > 0.01$; $n = 100$) (Figures 4D, 4G, and 4H). By contrast, cells overexpressing dnRok2 transplanted into a WT host did not elongate or acquire ML-biased orientation ($p < 1.6 \times 10^{-21}$ for LWR and $p < 0.001$ for ML alignment; $n = 92$) (Figures 4E, 4G, and 4H). These data indicate Rok2 function is required cell-autonomously for cell elongation and orientation. Labeled WT cells transplanted to a dnRok2 host elongated to a similar degree as untransplanted WT cells but were not mediolaterally oriented ($p > 0.1$ for LWR and $p < 0.001$; $n = 103$) (Figures 4F–4H). These mosaic analyses indicate that ML cell orientation may require both cell nonautonomous and cell-autonomous Rok2 activities. Intriguingly, both analyses of DiI-labeled and transplanted cells show that a cell can elongate independent of its ML orientation. According to previous models, as cells become ML oriented they exert traction on one another, leading to cell elongation; thus, predicting that acquisition of uniform ML cell orientation is a prerequisite for cell elongation [3]. Our study indicates cell elongation does not require concordant orientation of neighboring cells, as WT cells in a dnRok2-expressing host elongate without exhibiting ML bias. Accordingly, for dnRok2-expressing cells in a WT host, we found no correlation between elongation and ML-biased orientation of the cell body. This argues that mediolateral cell elongation in gastrulae is a more complex process requiring the intrinsic ability of individual cells to achieve/stabilize an elongated morphology in addition to reception and interpretation of cues from surrounding cells to acquire a ML-biased orientation.

Rok2 Is a Downstream Target of Noncanonical Wnt Signaling

DnRok2 disruption of CE within mesoderm and ectoderm without altering dorsal ventral patterning is strikingly similar to phenotypes reported for *slb/wnt11* and

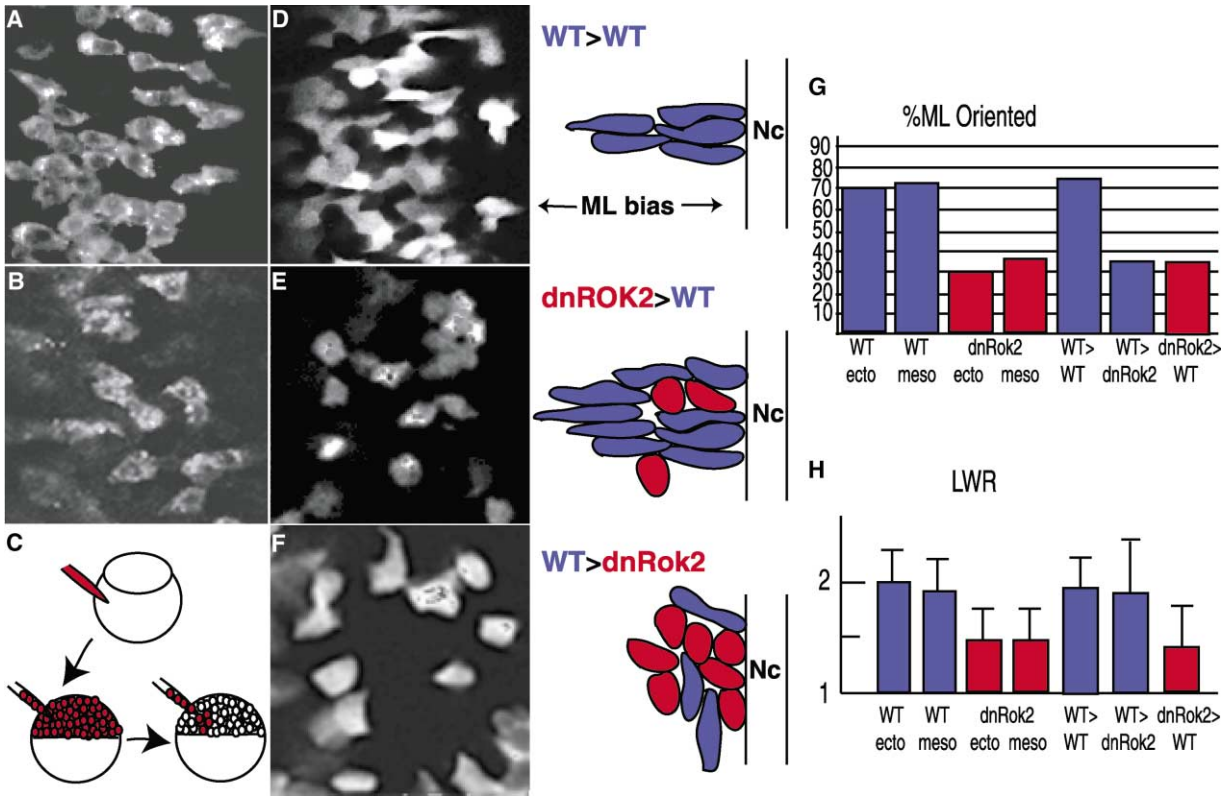

Figure 4. Rok2 Is Required Cell Autonomously and Nonautonomously for Polarized Cell Behaviors underlying CE

Confocal images of DiI-labeled (A) WT and (B) dnRok2-injected paraxial cells. (C) Rhodamine dextran alone or with dnRok2 was injected into 2 cell stage embryos. Labeled cells were transplanted at sphere stage into unlabeled WT or dnRok2-expressing hosts. Confocal and schematic images of transplanted WT (blue) or DnRok2 (red) cells. (D) WT cells are elongated and exhibit ML-biased orientation when transplanted into a WT host. (E) DnRok2 cells in a WT environment are neither elongated nor ML biased, while (F) WT cells in a dnRok2 host elongate but fail to acquire ML-biased orientation. (G) The percentage of WT and dnRok2 cells with their long axis oriented parallel to the mediolateral axis ± 20°. (H) Average length-width ratio (LWR) for labeled and transplanted WT and dnRok2 cells.

kny/gcp4/6 loss-of-function zebrafish mutants disrupting PCP signaling [4, 5]. These similarities and the recent findings that Drok acts downstream of Fz in *Drosophila* PCP signaling raise the possibility that during vertebrate gastrulation Rok2 acts downstream of Slb/Wnt11. To test this, we examined whether Rok2 can suppress the *slb*$^{-/-}$ gastrulation defects in molecular epistasis experiments. Impaired cell movements in homozygous *slb*$^{-/-}$ embryos lead to a posteriorly positioned and elongated prechordal plate and a broader neural plate and notochord compared to WT (Figures 5A and 5B) [32]. Increasing doses of *rok2* RNA reduced the fraction of *slb*$^{-/-}$ embryos exhibiting the strong mutant phenotype (Figures 5C and 5D). Similarly, at lower doses, Rok2 modestly suppressed the penetrance and expressivity of the *slb*$^{-/-}$ cyclopia phenotype but enhanced cyclopia at high doses (Figure 5E). While overexpression of Rok2 partially suppressed the CE phenotype, specifically, the width of the neural plate and the position of the prechordal plate, it does not rescue as efficiently as Wnt11. Furthermore, Rok2 overexpression does not eliminate the cyclopia phenotype, indicating a partial rescue. Therefore, additional factors are likely required to fully mediate Wnt11 function during CE. This is similar to findings in *Drosophila* which demostrated that DRok only mediates some aspects of PCP signaling downstream of Fz and Dsh [17]. In addition, we coexpressed dnRok2 and Wnt11 in homozygous *slb*$^{-/-}$ clutches to study further their functional interactions in CE. We found that injection of *wnt11* RNA efficiently rescues the *slb*$^{-/-}$ phenotype as previously reported [4], while injecting low doses of *dnRok2* neither enhances nor suppresses the *slb*$^{-/-}$ phenotype (Figure 5D). When *wnt11* and *dnRok2* RNAs were coinjected, only 72% of the *slb*$^{-/-}$ embryos were rescued, indicating that dnRok2 interferes with Wnt11 function (Figure 5D). Together, these data suggest Rok2 acts downstream or parallel to Slb/Wnt11 during CE.

Rok2 activity has been correlated with its intracellular distribution in cultured cells, where the active kinase localizes near the cell membrane [18]. If Rok2 is an effector of Wnt signaling, then Wnt overexpression should influence Rok2 intracellular localization (Figure 6A). In WT or rat Rok2-HA overexpressing zebrafish blastula Rok2 is localized to cell membranes ($n = 10$ embryos); this localization is not detected with secondary antibody alone (Figures 6B–6D). Notably, overexpression of Wnt5/Ppt ($n = 6$ embryos) or Wnt11/Slb ($n = 6$ embryos) at high doses sufficient to disrupt CE results in cytoplasmic Rok2 distribution and likely its inactivation (Figures 6E and 6F). To determine whether canonical Wnts could also modulate Rok2 intracellular distribution

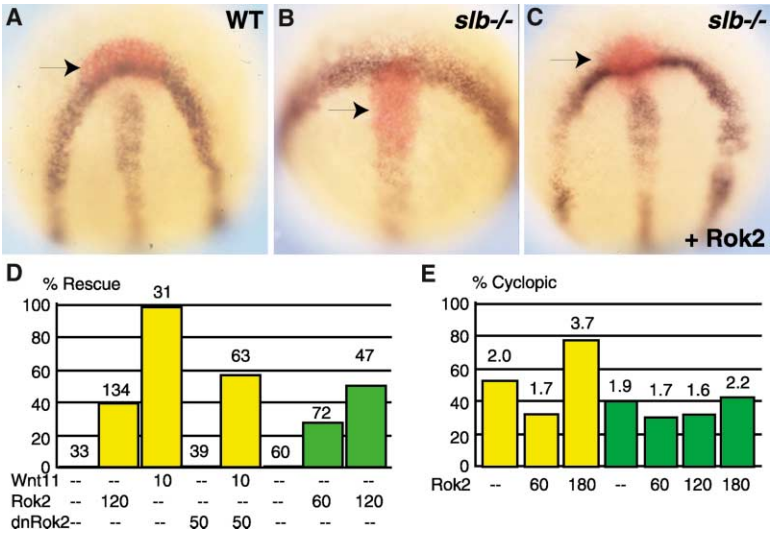

Figure 5. Rok2 Suppresses the *slb/wnt11* Mutant Phenotype

(A and B) Dorsal-animal views of (A) WT embryo, arrow indicates positioning of the hatching gland (*hgg1*) (red) rostral to the anterior-most edge of the neural plate (*dlx3*), while midline (*shh*) extends to the edge of the np. (B) *slb*$^{-/-}$ embryo; the prechordal plate is elongated and positioned posterior to the np (arrow), and the midline is short and broad. (C) In *slb*$^{-/-}$ embryo injected with full-length *rok2* RNA, the prechordal plate migration defect is suppressed (arrow). (D) Percentage of rescued embryos derived from homozygous *slb*$^{-/-}$ parents as judged by the position of the prechordal plate and coinjection of *dnrok2* RNA interferes with Wnt11 rescue of the *slb/wnt11* mutant phenotype (number above bar indicates number of *slb*$^{-/-}$). (E) The percent penetrance and expressivity determined by calculating the cyclopia index (indicated above bars) [36] for embryos obtained from homozygous *slb*$^{-/-}$ parents.

we injected synthetic *wnt8* RNA [33]. In contrast to noncanonical Wnt overexpression, Rok2 is membrane localized in embryos overexpressing Wnt8, indicating this canonical Wnt either promotes membrane localization or fails to influence Rok2 (n = 9 embryos) (Figure 6G). Similar results were obtained when HA-tagged ratRok2 localization was monitored with a monoclonal HA antibody (data not shown). Displacement of Rok2 from the membrane and likely its inactivation is consistent with observations that both gain and loss of morphogenetic Wnt function disrupt morphogenesis [4, 11, 13, 34]. Cumulatively, these genetic and molecular experiments indicate that Rok2 is a target of noncanonical Wnt signaling.

Conclusions

In summary, the genes and distinct cellular behaviors underlying convergence and extension movements during vertebrate gastrulation are beginning to be elucidated [4, 5, 28]. Here we cloned zebrafish *rok2* and showed that it is expressed in a manner consistent with a role in regulating cell behaviors underlying gastrulation. We demonstrate that Rok2 function is required for normal convergence and extension movements but not for cell fate specification events in the zebrafish gastrula as reported for *slb* and *kny* mutants [4, 5]. We present evidence that cell polarization is disrupted in dnRok2-expressing embryos and propose that defective cell polarization impedes effective movement along straight

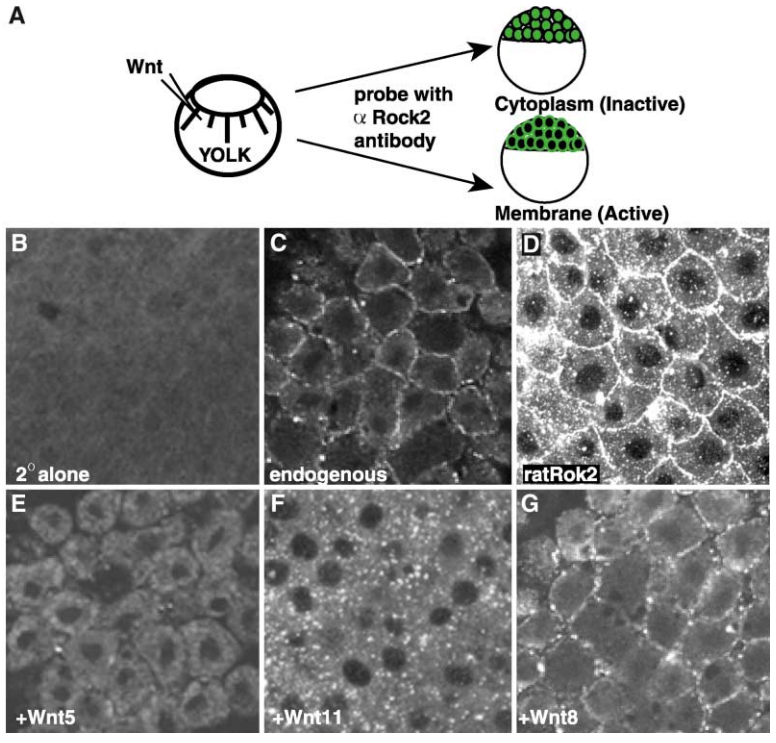

Figure 6. Rok2 Is a Target of Noncanonical Wnt Signaling

(A) Schematic of Rok2 translocation assay, membrane-associated (associated with active Rok2) or localized to the cytoplasm (associated with inactive Rok2). (B–G) Confocal images. (B) 2° antibody alone. Rok2 is membrane localized (C) endogenously and (D) in embryos overexpressing rat Rok2. (E) Wnt5 or (F) Wnt11 overexpression promotes cytoplasmic distribution of Rok2 protein. (G) In contrast, Rok2 is membrane localized in embryos overexpressing Wnt8.

paths and consequently impairs CE. Specifically, Rok2 is required cell-autonomously for cell elongation; however, ML-biased orientation depends on cell-autonomous and nonautonomous Rok2 function. Cells in the gastrula can elongate regardless of their orientation, indicating that even though these behaviors are always coexpressed during CE, cell elongation and orientation are independent cell properties. Finally, we show for the first time that Rok2 acts downstream of Wnt11-mediated vertebrate tissue polarity signaling pathway, linking the ligand to an intracellular modulator of cell behavior.

Experimental Procedures

Zebrafish Maintenance, Embryo Generation, and Staging

AB* and TL WT and *slb*$^{-/-}$ zebrafish strains were maintained as described in [35]. Embryos were obtained from natural spawnings and staged according to morphology as described in [24].

Cloning and Sequencing of rok2

Two zebrafish-expressed sequence tag (EST) clones corresponding to the *rok2* gene (GenBank accession numbers AI545209 and AA658629) were identified (Research Genetics), and the missing internal fragment was isolated using RT-PCR. The complete coding sequence was subcloned into the pCS2 vector and sequenced. Dn*Rok2* was generated by digesting the full-length *Rok2* with XbaI and ApaI and subcloning to pCS2.

In Situ Hybridization

Sense and antisense probes were synthesized as described [36], using the amino-terminal and carboxy-terminal EST clones as templates. After comparing expression for both fragments, the carboxy-terminal EST was used for further analysis. Antisense probe synthesis for *dlx3* [37], *hgg1* [38], *ntl* [39], *shh* [40], *bmp4* [41], and *papc* [42] was as described [25, 36]. Whole-mount in situ hybridization was performed according to [43], except malic acid buffer with 0.01% Tween 20 and levamisole was used to prepare NTMT stain buffer, and BM purple (Roche) was used for *rok2* staining.

RNA Injections

Capped sense RNA encoding Rok2 or dnRok2 was synthesized with SP6 RNA polymerase (Ambion mMessage Machine system). Wnt11, Wnt 8, and Wnt5 and membrane-localized GFP were used as templates as described in [34]. RNA injections were performed according to [36].

Rok2 Morpholino Injections

Two distinct MO oligonucleotides targeted to the 5′-UTR (CTGCTCAACTTTTCTGGTTTACATT) and overlapping the first ATG (CTCCTAGCGACATTTTTGTCTCGT) of the *rok2* gene were used. When injected alone, neither MO produced a phenotype at doses ranging from 2 to 24 ng/embryo. When the MO oligonucleotides were injected together, we found some defects at doses 16, 24, and 32 ng, including CNS degeneration. The penetrance of these defects increased in a dose-dependent manner; however, these defects could not be rescued by injecting ratRok2 mRNA.

Cell Labeling/Lineage Analysis

Were performed as described in [25], except embryos were injected with dnRok2 prior to cell labeling.

Cell Polarity and Rok2 Autonomy

Scatter labeling with DiI in control and dnRok2-expressing embryos was as described [5]. Z series images were acquired between bud and 1 somite stages at 3 μm intervals using the Zeiss LSM 410 confocal microscope (supported by NIH grants CA68485 and DK20593), and cell orientation and LWR were determined according to [5]. For cell autonomy analyses, embryos were labeled with biotinylated Rhodamine dextran instead of DiI. Labeled control and dnRok2-expressing cells were transplanted as described in [44] into unlabeled control or dnRok2-expressing hosts at midblastula stage. Between bud and 1 somite stages, confocal Z series were obtained, and cell orientation and LWR were measured according to [5]. Statistical analysis was performed as described in [5].

Nomarski Time-Lapse

Nomarski time-lapse within the mesoderm were obtained using the Zeiss Axiophot microscope and digital Axiocam camera. The centers for individual cells were determined using NIH Image 1.62. Cell migration paths, speeds, and P values were calculated using Microsoft Excel.

Immunostaining

Embryos were injected with RNA encoding HA-ratRok2 alone or with Wnt11, Wnt5, or Wnt8, fixed and stained as described [5], except the following antibodies were used: the primary antibody C20 anti-Rok2 polyclonal antibody (1:100) (Research Antibodies) and anti-goat IgG secondary antibody conjugated to Alexa green 488 (1:250) (Molecular Probes). To monitor HA-tagged rat Rok2 localization, anti-HA primary antibody (1:250) (Sigma) and anti-mouse IgG secondary antibody conjugated to CY3 (1:250) (Jackson Immuno) were used. Images were acquired using the Zeiss LSM 410 or 510 laser scanning inverted microscope.

Acknowledgments

We thank L. Lim for rat HA-tagged full-length Rok and RokK112A constructs. We thank P. Ingham for *shh*; M. Ekker for *dlx3*; D. Grunwald for *gsc*; N. Ueno for *bmp4* clones; and C.-P. Heisenberg for *slb* mutant fish. We thank A. Schier and E. Raz for kindly providing helpful comments. We thank J. Clanton for excellent fish care. F.M. is supported by a National Institutes of Health Developmental Biology training grant and D.S.S. by a NIH Vascular Biology training grant (T32HL07751); work in L.S.-K. lab is supported by NIH GM55101 and Pew Scholars Program in Biomedical Sciences.

Received: January 28, 2002
Revised: April 5, 2002
Accepted: April 15, 2002
Published: June 4, 2002

References

1. Keller, R., Clark, W.H., Jr., and Griffin, F. (1991). Gastrulation. Movements, patterns, and molecules. Marine Science Series (New York: Plenum Press).
2. Warga, R.M., and Kimmel, C.B. (1990). Cell movements during epiboly and gastrulation in zebrafish. Development *108*, 569–580.
3. Keller, R., Davidson, L., Edlund, A., Elul, T., Ezin, M., Shook, D., and Skoglund, P. (2000). Mechanisms of convergence and extension by cell intercalation. Philos. Trans. R. Soc. Lond. B Biol. Sci. *355*, 897–922.
4. Heisenberg, C.P., Tada, M., Rauch, G.J., Saude, L., Concha, M.L., Geisler, R., Stemple, D.L., Smith, J.C., and Wilson, S.W. (2000). Silberblick/Wnt11 mediates convergent extension movements during zebrafish gastrulation. Nature *405*, 76–81.
5. Topczewski, J., Sepich, D.S., Myers, D.C., Walker, C., Amores, A., Lele, Z., Hammerschmidt, M., Postlethwait, J., and Solnica-Krezel, L. (2001). The zebrafish glypican knypek controls cell polarity during gastrulation movements of convergent extension. Dev. Cell *1*, 251–264.
6. Wallingford, J.B., Rowning, B.A., Vogeli, K.M., Rothbacher, U., Fraser, S.E., and Harland, R.M. (2000). Dishevelled controls cell polarity during *Xenopus* gastrulation. Nature *405*, 81–85.
7. Mlodzik, M. (1999). Planar polarity in the Drosophila eye: a multifaceted view of signaling specificity and cross-talk. EMBO J. *18*, 6873–6879.
8. Sokol, S. (2000). A role for Wnts in morpho-genesis and tissue polarity. Nat. Cell Biol. *2*, E124–E125.
9. Tada, M., and Smith, J.C. (2000). Xwnt11 is a target of *Xenopus* Brachyury: regulation of gastrulation movements via Dishevelled, but not through the canonical Wnt pathway. Development *127*, 2227–2238.

10. Deardorff, M.A., Tan, C., Conrad, L.J., and Klein, P.S. (1998). Frizzled-8 is expressed in the Spemann organizer and plays a role in early morphogenesis. Development *125*, 2687–2700.
11. Moon, R.T., Campbell, R.M., Christian, J.L., McGrew, L.L., Shih, J., and Fraser, S. (1993). Xwnt -5A: a maternal Wnt that affects morphogenetic movements after overexpression in embryos of *Xenopus laevis*. Development *119*, 91–111.
12. Sokol, S.Y. (1996). Analysis of Dishevelled signalling pathways during *Xenopus* development. Curr. Biol. *6*, 1456–1467.
13. Ungar, A.R., Kelly, G.M., and Moon, R.T. (1995). Wnt4 affects morphogenesis when misexpressed in the zebrafish embryo. Mech. Dev. *52*, 153–154.
14. Mlodzik, M. (2000). Spiny legs and prickled bodies: new insights and complexities in planar polarity establishment. Bioessays *22*, 311–315.
15. Djiane, A., Riou, J., Umbhauer, M., Boucaut, J., and Shi, D. (2000). Role of frizzled 7 in the regulation of convergent extension movements during gastrulation in Xenopus laevis. Development *127*, 3091–3100.
16. Habas, R., Kata, Y., and He, X. (2001). Wnt/Frizzled activation of Rho regulates vertebrate gastrulation and requires a novel formin homology protein Daam1. Cell *107*, 1–20.
17. Winter, C.G., Wang, B., Ballew, A., Royou, A., Karess, R., Axelrod, J.D., and Luo, L. (2001). *Drosophila* Rho-associated kinase (Drok) links Frizzled-mediated planar cell polarity signaling to the actin cytoskeleton. Cell *105*, 81–91.
18. Leung, T., Chen, X.Q., Manser, E., and Lim, L. (1996). The p160 RhoA-binding kinase ROK alpha is a member of a kinase family and is involved in the reorganization of the cytoskeleton. Mol. Cell. Biol. *16*, 5313–5327.
19. Wissmann, A., Ingles, J., McGhee, J.D., and Mains, P.E. (1997). Caenorhabditis elegans LET-502 is related to Rho-binding kinases and human myotonic dystrophy kinase and interacts genetically with a homolog of the regulatory subunit of smooth muscle myosin phosphatase to affect cell shape. Genes Dev. *11*, 409–422.
20. Wei, L., Roberts, W., Wang, L., Yamada, M., Zhang, S., Zhao, Z., Rivkees, S.A., Schwartz, R.J., and Imanaka-Yoshida, K. (2001). Rho kinases play an obligatory role in vertebrate embryonic organogenesis. Dev. Suppl. *128*, 2953–2962.
21. Ishizaki, T., Naito, M., Fujisawa, K., Maekawa, M., Watanabe, N., Saito, Y., and Narumiya, S. (1997). p160ROCK, a Rho-associated coiled-coil forming protein kinase, works downstream of Rho and induces focal adhesions. FEBS Lett. *404*, 118–124.
22. Amano, M., Chihara, K., Nakamura, N., Kaneko, T., Matsuura, Y., and Kaibuchi, K. (1999). The COOH terminus of Rho-kinase negatively regulates rho-kinase activity. J. Biol. Chem. *274*, 32418–32424.
23. Amano, M., Fukata, Y., and Kaibuchi, K. (2000). Regulation and functions of Rho-associated kinase. Exp. Cell Res. *261*, 44–51.
24. Kimmel, C.B., Ballard, W.W., Kimmel, S.R., Ullmann, B., and Schilling, T.F. (1995). Stages of embryonic development of the zebrafish. Dev. Dyn. *203*, 253–310.
25. Sepich, D.S., Myers, D.C., Short, R., Topczewski, J., Marlow, F., and Solnica-Krezel, L. (2000). Role of the zebrafish trilobite locus in gastrulation movements of convergence and extension. Genesis *27*, 159–173.
26. Verde, F., Wiley, D.J., and Nurse, P. (1998). Fission yeast orb6, a ser/thr protein kinase related to mammalian rho kinase and myotonic dystrophy kinase, is required for maintenance of cell polarity and coordinates cell morphogenesis with the cell cycle. Proc. Natl. Acad. Sci. USA *95*, 7526–7531.
27. Yasui, Y., Amano, M., Nagata, K., Inagaki, N., Nakamura, H., Saya, H., Kaibuchi, K., and Inagaki, M. (1998). Roles of Rho-associated kinase in cytokinesis: mutations in Rho-associated kinase phosphorylation sites impair cytokinetic segregation of glial filaments. J. Cell Biol. *143*, 1249–1258.
28. Myers, D.C., Sepich, D.S., and Solnica-Krezel, L. (2002). Bmp activity gradient regulates convergence and extension during zebrafish gastrulation. Dev. Biol. *243*, 81–98.
29. Hammerschmidt, M., Serbedzija, G.N., and McMahon, A. (1996). Genetic analysis of dorsoventral pattern formation in the zebrafish: requirement of BMP-like ventralizing activity and its dorsal repressor. Genes Dev. *10*, 2452–2461.
30. Concha, M., and Adams, R. (1998). Oriented cell divisions and cellular morphogenesis in the zebrafish gastrula and neurula: a time-lapse analysis. Development *125*, 983–994.
31. Trinkaus, J.P. (1992). The midblastula transition, the YSL transition and the onset of gastrulation in fundulus. Dev. Suppl., 75–80.
32. Heisenberg, C.P., and Nusslein-Volhard, C. (1997). The function of *silberblick* in the positioning of the eye anlage in the zebrafish embryo. Dev. Biol. *184*, 85–94.
33. Miller, J.R., Hocking, A.M., Brown, J.D., and Moon, R.T. (1999). Mechanism and function of signal transduction by the Wnt/beta-catenin and Wnt/Ca^{2+} pathways. Oncogene *18*, 7860–7872.
34. Makita, R., Mizuno, T., Kuroiwa, A., Koshida, S., and Takeda, H. (1998). Zebrafish wnt11: pattern and regulation of the expression by the yolk cell and no tail activity. Mech. Dev. *71*, 165–176.
35. Solnica-Krezel, L., Schier, A.F., and Driever, W. (1994). Efficient recovery of ENU-induced mutations from the zebrafish germline. Genetics *136*, 1401–1420.
36. Marlow, F., Zwartkruis, F., Malicki, J., Neuhauss, S.C.F., Abbas, L., Weaver, M., Driever, W., and Solnica-Krezel, L. (1998). Functional interactions of genes mediating convergent extension, *knypek* and *trilobite*, during partitioning of the eye primordium in zebrafish. Dev. Biol. *203*, 382–399.
37. Akimenko, M.A., Ekker, M., Wegner, J., Lin, W., and Westerfield, M. (1994). Combinatorial expression of three zebrafish genes related to distal-less: part of a homeobox gene code for the head. J. Neurosci. *14*, 3475–3486.
38. Thisse, C., Thisse, B., Halpern, M.E., and Postlethwait, J.H. (1994). Goosecoid expression in neurectoderm and mesendoderm is disrupted in zebrafish cyclops gastrulas. Dev. Biol. *164*, 420–429.
39. Schulte-Merker, S., Ho, R.K., Herrmann, B.G., and Nusslein-Volhard, C. (1992). The protein product of the zebrafish homologue of the mouse T gene is expressed in nuclei of the germ ring and the notochord of the early embryo. Development *116*, 1021–1032.
40. Krauss, S., Concordet, J.P., and Ingham, P.W. (1993). A functionally conserved homolog of the Drosophila segment polarity gene hh is expressed in tissues with polarizing activity in zebrafish embryos. Cell *75*, 1431–1444.
41. Nikaido, M., Tada, M., Saji, T., and Ueno, N. (1997). Conservation of BMP signaling in zebrafish mesoderm patterning. Mech. Dev. *61*, 75–88.
42. Yamamoto, A., Amacher, S.L., Kim, S.H., Geissert, D., Kimmel, C.B., and De Robertis, E.M. (1998). Zebrafish *paraxial protocadherin* is a downstream target of spadetail involved in morphogenesis of gastrula mesoderm. Development *125*, 3389–3397.
43. Thisse, C., and Thisse, B. (1998). High Resolution Whole-Mount in situ Hybridization. Zebrafish Science Monitor *5*, 3389–3397.
44. Westerfield, M. (1996). The Zebrafish Book: A Guide for the Laboratory Use of Zebrafish (*Danio rerio*) (Eugene, OR: University of Oregon Press).

Accession Numbers

The *rok2* gene sequence reported in this paper can be found in GenBank under the accession number AF295804.